Physics of the Earth and Planetary Interiors 240 (2015) 25–33

Contents lists available at ScienceDirect

Physics of the Earth and Planetary Interiors

journal homepage: www.elsevier.com/locate/pepi

A timescale of true polar wander of a quasi-fluid Earth: An effect of a low-viscosity layer inside a mantle

Yuji Harada *, Long Xiao

Planetary Science Institute, School of Earth Sciences, China University of Geosciences (Wuhan), 388 Lumo Road, Hongshan District, Wuhan City, Hubei Province 430074, China

ARTICLE INFO

Article history:
Received 10 April 2014
Received in revised form 7 October 2014
Accepted 4 November 2014
Available online 18 November 2014

Keywords:
True polar wander
Quasi-fluid approximation
Characteristic timescale
Earth
Mantle
Low-viscosity layer

ABSTRACT

By means of a simple parameter sensitivity analysis, we demonstrate the effect of a low-viscosity layer inserted inside a mantle of a hypothetical Earth on the timescale of large-scale and long-term true polar wander. Here the timescale in our parameter study means the characteristic scale of viscoelastic readjustment of the rotational bulge in the framework of the quasi-fluid approximation for the long-term reorientation of the Earth. Based on this assumption, we calculate the characteristic timescale and associated viscoelastic tidal Love number with the effect of this layer in order to see the dependences on the viscosity, depth, and thickness of the inserted layer. We also compute the characteristic timescale without this layer for the sake of comparison. Our results indicate that the timescale strongly depends on the existence of this layer: positive dependences on its viscosity and depth and a negative dependence on its thickness. We conclude that the low-viscosity layer has a strong impact on the characteristic timescale, especially if this layer exists at the top of the mantle. Although a few previous studies on the small-scale and short-term true polar wander have also suggested a possible effect of inserting a low-viscosity layer, our study implies that the sensitivity to the low-viscosity layer over a long timespan is not necessarily the same as that over a short timespan.

1. Introduction

1.1. Background

Large-scale and long-term true polar wander (TPW) on the terrestrial planets, particularly the Earth and Mars, has been theoretically and numerically investigated by several studies. Some of the studies on the large-scale TPW (Spada et al., 1992a; Spada et al., 1993; Spada et al., 1996; Ricard et al., 1993; Richards et al., 1997; Richards et al., 1999; Greff-Lefftz, 2004; Greff-Lefftz, 2011; Tsai and Stevenson, 2007; Rouby et al., 2008) are based on the quasi-fluid approximation whereas the others (Nakada, 2007; Nakada, 2008) are based on the iteration scheme, in order to solve the polar motion equation, or the so-called Liouville equation (Munk and MacDonald, 1960; Lambeck, 1980), in the form of the non-linear equation. A few recent studies based on the former approach (Harada, 2012; Creveling et al., 2012; Chan et al., 2014) even consider the stabilizing effect of non-hydrostatic figures memorized in elastic lithospheres (e.g., Willemann, 1984; Matsuyama et al., 2006).

These theoretical and numerical studies on the large-scale TPW are considered essential for a quantitative understanding of actual long-term rotational evolution. For example, mainly based on paleomagnetic circumstantial evidence, possible TPW events on the Earth (e.g., Van der Voo, 1994; Maloof et al., 2006; Steinberger and Torsvik, 2008; Mitchell et al., 2010a; Mitchell et al., 2010b; Torsvik et al., 2012) and Mars (e.g., Sprenke and Baker, 2000; Hood et al., 2005; Boutin and Arkani-Hamed, 2006; Langlais and Quesnel, 2008) have been inferred. Such large-scale TPW scenarios needs to be interpreted theoretically as well. The above-mentioned TPW modeling enables us to physically examine their validity (e.g., Creveling et al., 2012).

The reconstruction of the physical conditions which explain the hypothetical TPW events is expected to further put some additional constraints on past thermal states of the planets. This is because the TPW speed generally depends on the internal structure, especially the viscosity structure. In particular, in the case of the long-term TPW, one of the factors governing its speed is T_1 (see the next section), that is, the characteristic timescales of readjustment of the rotational bulge. This factor is determined by the viscoelastic relaxation modes of the tidal Love number (e.g., Peltier, 1974; Wu and Peltier, 1982), and hence, by the viscosity structure.

* Corresponding author.
E-mail address: harada@cug.edu.cn (Y. Harada).

http://dx.doi.org/10.1016/j.pepi.2014.11.001
0031-9201/

In the conventional modeling of the large-scale TPW, heterogeneity on the viscosity structure of the mantle in terms of a potential impact of a low-viscosity layer (LVL), has not necessarily been dealt with. In fact, a large variety of geophysical observations tells us that the Earth's interior may include one layer or more with a large viscosity difference between its inside and outside, inserted at the upper (e.g., Klein et al., 1997; Forte and Mitrovica, 2001; Pollitz, 2003; Hearn, 2003; Dixon et al., 2004; Mitrovica and Forte, 2004; Steffen and Kaufmann, 2005; Kawakatsu et al., 2009) and/or lower (e.g., Nakada and Karato, 2012; Nakada et al., 2012) part(s) of the mantle. In addition to the Earth's mantle, there is a similar possibility that the Mars' mantle also possesses this kind of remarkable viscosity contrast based on tidal dissipation (Bills et al., 2005) and also the numerical simulation of the mantle convection with the influence of water inclusion (Ogawa and Yanagisawa, 2012). Nevertheless, in the previous studies, the viscosity structure has been roughly averaged, and therefore, assumed to include no mechanically-specific layer as above.

A few exceptional studies investigated the potential impact of the LVL on relatively small-scale and short-term TPW induced by the glacial isostatic adjustment (GIA). The exceptions are Milne et al. (1998) and Nakada and Okuno (2013), each of which explored the effect of the LVL inserted at the base of the upper or lower part of the mantle, respectively, on the secular rotational variation of the Earth. The impact of a shallower LVL on the TPW speed is small while that on the secular variation of the rotation rate (i.e., $\dot{J_2}$) is large. In contrast, the impact of a deeper LVL on the TPW speed is large while that on $\dot{J_2}$ is small. Although the spatial and temporal scales of the TPW in their studies are not the same as those addressed here, it is considered to be possible that the LVL at some depth also has a non-negligible influence on the speed of the large-scale TPW.

1.2. Purpose

In this paper, we show how the characteristic timescale of the large-scale TPW depends on the viscosity, depth, and thickness of the LVL inside the mantle, by giving the internal structure of a simplified Earth model, but with inclusion of an LVL effect. Here we suppose the long-term TPW which timescale allow us to apply the quasi-fluid approximation. Because the TPW speed strongly depends on the parameter T_1 for such a timescale as described above, we focus on the dependence of T_1 on the interior structure.

2. Parameters & methods

2.1. The characteristic timescale of readjustment of the rotational bulge (T_1)

Under a timescale long enough to allow the quasi-fluid approximation, the magnitude of T_1 represents the viscoelastic delay of the hydrostatic readjustment with respect to the excursion of the spin pole. The definition of T_1 has been described in several papers, such as Eq. (8) in Ricard et al. (1993), Eq. (3) in Spada et al. (1996), and Eq. (5) in Greff-Lefftz (2004). This value has a dimension of time and, in the case of the long-term TPW as mentioned in here, affects the timescale in which the rotation axis settles to the equilibrium position.

Regardless of the presence or absence of the stabilizing effect due to the non-hydrostatic form, T_1 is one of the important controlling factors to understand the characteristic timescale of the large-scale and long-term TPW. For example, in both cases, the non-linear Liouville equation is simplified as Eq. (82) in Harada (2012) for an axially symmetric load. This equation makes it clear that, for a certain load evolution, a larger T_1 results in a slower TPW. This tendency is even more obvious in the analytic solution for a linearly increasing load, for example, shown in Eq. (7) in Spada et al. (1996) and Eq. (100) in Harada (2012) for the case without the non-hydrostatic effect. In such a simple load formation, the TPW timescale is mostly proportional to T_1 if the timescale of the load formation is relatively short (if not, the viscoelastic delay related to T_1 is no longer dominant, and thus the TPW timescale is controlled by the loading timescale). This point is nearly the same even considering the non-hydrostatic effect due to the elastic lithosphere as in Eq. (103) in Harada (2012).

The objective of the present calculation is mainly to clarify the sensitivity of this T_1 value to the LVL effect. As in the definition cited above, T_1 is not simply expressed as the sum of the relaxation timescales (i.e., $-1/s_i$) of the viscoelastic modes. Rather, in T_1, each of the relaxation timescales is associated with its relaxation strength (i.e., $-k_i/s_i$) for tidal deformation assigned as a weighting factor. As a consequence, T_1 is not generally equal to the viscoelastic timescale of the tidal deformation itself although a uniform Newtonian (not Maxwellian) planetary body is an exceptional case (e.g., Tsai and Stevenson, 2007) as derived in Appendix A.3 of Harada (2012). All of the timescales and strengths for the relaxation modes reflect the internal structure, that is, the density, elasticity, and viscosity profiles. This structure dependence of T_1, especially on the viscosity structure, is investigated by defining the parameter sets as described below.

It should be mentioned here that any driving force for TPW is out of scope in the present study. In fact, as shown in Eq. (16) in Ricard et al. (1993) and Eq. (1) in Spada et al. (1996), the timescale is directly proportional to the difference between the maximum and minimum moment of inertia $C - A$ as well as T_1, and also inversely proportional to excitation E. That is, the real time constant of TPW is $T_1(C - A)/E$ rather than T_1. In general, depending on how large this normalized excitation $E/(C - A)$ is, the actual TPW timescale is a few orders of magnitude longer than T_1. However, as mentioned already, the aim of this study is to focus just on T_1 under the LVL effect. Therefore, $E/(C - A)$ is not discussed in here.

2.2. Invariable parameters: Density and elasticity profiles

The baseline density and elasticity structure model of the Earth for the present calculation is given in Table 1. This is exactly the same as that used in Bills and James (1997), following those originally used in Yuen et al. (1983) and Sabadini et al. (1984). See Table 1 of Bills and James (1997), although the viscosity structure in their table corresponds to the model Y2121 in their notation, not Y2122 as shown in Table 1 in here. For numerical convenience, as in this table, a largely simplified model compared to more realistic models (cf., Gilbert and Dziewonski, 1975; Dziewonski and Anderson, 1981) is assumed in the computation. Also, assumed for each solid layers are incompressible media, and therefore only rigidity is given as an elastic modulus. However, this simplification does not necessarily affect the validity of the subsequent discussion since the main aim at the current time is just to see the potential impact of the LVL.

2.3. Variable parameters: Viscosity profiles

The baseline viscosity structure model of the Earth for the present calculation is also given in Table 1. This is exactly the same as that defined in Nakada and Karato (2012). See R0 shown in Fig. 1 of Nakada and Karato (2012). Once again, for the sake of the calculation based on the assumption of incompressibility, the viscosity profile is simplified as well as the density and elasticity profiles, except for the presence of the LVL as mentioned below. In this

Table 1
The baseline interior structure model adopted in the present study, where the rheological boundaries are assumed to be the same as the chemical ones.

Y2122	Radius (km)	Density (kg m^{-3})	Rigidity (GPa)	Viscosity (Pa s)
Crust	6371	2771	31.5	Infinity
Mantle				
Upper	6271	4120	95.4	10^{21}
Lower	5701	4508	199.0	10^{22}
Core	3480	10925	0	

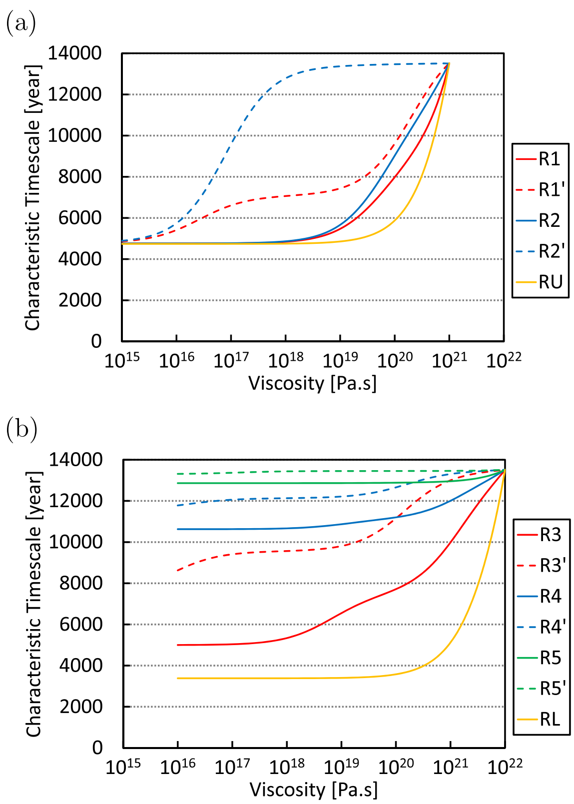

Fig. 1. (a) Dependence of the characteristic timescale T_1 of true polar wander on viscosity of a low-viscosity part inserted into the upper mantle. The different curves represent the different low-viscosity models defined in Table 2. (b) Same as (a) but with a low-viscosity part inside the lower mantle.

viscoelasticity structure model in Table 1, the rheological boundaries between the lithosphere and asthenosphere and the asthenosphere and mesosphere are implicitly assumed to be the same as the chemical ones between the crust and mantle and the upper and lower mantle, respectively.

The LVL models inserted into the above baseline model are given in Table 2. Among them, the depth ranges of R1 to R5 are exactly the same as those defined in Nakada and Karato (2012). See R1 to R5 shown in Table 1 of Nakada and Karato (2012), although the viscosity ranges in their table are not the same as those shown in Table 2. Since the most important key is the dependence on the viscosity of the LVL, these viscosity values cover wide ranges of six orders of magnitude. In addition to R1 to R5, much thinner LVL models with the same viscosity ranges are also taken into account for considering the effect of a thinner thickness. Each thickness of the thinner models R1′ to R5′ is one-tenth that of R1 to R5, respectively. More extreme models RU and RL are also considered such that either of the viscosity over the whole upper or lower mantle is uniformly reduced. Although not all of the various models are realistic, it is still worth considering also unrealistic cases for a better physical understanding.

By using these viscosity profiles, in conjunction with the density and elasticity profiles, the viscoelastic tidal Love number is numerically derived for each internal structure. A suite of the relaxation modes corresponding to each viscosity profiles is computed via the normal mode method (e.g., Peltier, 1974; Wu and Peltier, 1982), especially by using the fundamental matrix (e.g., Spada et al., 1992b; Vermeersen et al., 1996) for incompressible deformation. The number of the relaxation modes computed here is four times the number of the viscoelastic layers. For example, twelve and sixteen modes are estimated for R1 (with three viscoelastic layers) and R2′ (with four viscoelastic layers), respectively. Among all of the modes found in here, any mode with a negative strength is regarded as a computational mode with no physical meaning, and is therefore ignored. In addition to such non-physical modes, any mode with a timescale longer than ten billion years is also negligible since it will never relax within a realistic timespan. Although the exclusion of these modes slightly changes the fluid Love number, the impact of this slight change on T_1 is negligibly small, and therefore is not considered in here.

3. Results

3.1. Dependence on the viscosity structure of the upper mantle

The effect of the low-viscosity structure in the upper mantle is shown in Fig. 1 (a). The calculation results clearly demonstrate strong dependence of T_1 on the presence of the LVL, particularly the positive dependences on its viscosity and depth and the negative dependence on its thickness. In particular, the shallowest LVL models (i.e., R1 and R1′) dramatically reduce the T_1 timescale. For example, even if the LVL viscosity is only two to three orders of magnitude smaller than the baseline viscosity, the T_1 timescale becomes less than about a half of that for the baseline model. In addition, each curve converges to a constant T_1 value for the lower viscosity side, which is almost the same as that of the RU model. Also for the higher viscosity side, all of these curves converge into the other constant T_1 value as each viscosity value approaches its maximum value. The latter convergence results solely from the present parameter setting, in which the maximum values of the viscosity ranges for all of the LVL models are defined as the same as that of the baseline model.

3.2. Dependence on the viscosity structure of the lower mantle

The effect of the low-viscosity structure in the lower mantle is shown in Fig. 1 (b). The structure dependence on the lower mantle is basically the same as that on the upper mantle as described above. However, the dependence of T_1 on the depth is much greater, especially for the low viscosity side, where there is no convergence. For example, the R3 model indicates the T_1 value which is relatively close to that of the RL model for the lower viscosity side whereas the R5 model indicates no significant sensitivity.

4. Discussion & conclusions

4.1. Physical interpretation on the present results

The present calculation results indicates that, for any LVL inside a planetary body, a lower LVL viscosity corresponds to a faster TPW speed. The reason of this tendency would be because the presence of the LVL shortens the relaxation timescales of the viscoelastic modes on the whole. In addition to the viscosity, if the LVL becomes thicker, the relative strength of the short-term and

Table 2
A low-viscosity part inserted into the baseline model.

(a) A multi-layered mantle with a thick low-viscosity layer				
R1–R5			Depth (km)	Viscosity (Pa s)
Mantle	Upper	R1	100–400	10^{15}–10^{21}
		R2	400–670	
	Lower	R3	791–1091	10^{16}–10^{22}
		R4	1691–1991	
		R5	2591–2891	
(b) A multi-layered mantle with a thin low-viscosity layer				
R1′–R5′			Depth (km)	Viscosity (Pa s)
Mantle	Upper	R1′	100–130	10^{15}–10^{21}
		R2′	400–427	
	Lower	R3′	1061–1091	10^{16}–10^{22}
		R4′	1961–1991	
		R5′	2861–2891	
(c) A two-layered mantle with no low-viscosity layer				
RU & RL			Depth (km)	Viscosity (Pa s)
Mantle	Upper	RU	100–670	10^{15}–10^{21}
	Lower	RL	670–2891	10^{16}–10^{22}

long-term relaxation modes would become larger and smaller, respectively. As a result, the inertia tensor variation with respect to the centrifugal potential perturbation due to the TPW becomes faster as well, and thus the characteristic timescale following the excursion of the spin pole becomes shorter. In particular, if the LVL viscosity is sufficiently low, this layer is considered to practically behave as a liquid layer in terms of the TPW speed. Under such a condition, because the viscoelastic properties of this liquid-like layer has no further contribution to T_1, the T_1 value gets close to the constant timescale with varying LVL viscosity regardless of its LVL thickness. This is probably the main reason why the T_1 curves for the LVL models with the same depth (i.e., R1 and R1′, and also R2 and R2′) asymptotically approach the same value in the results for a variable upper mantle structure.

The results also indicates that a shallower LVL depth corresponds to a faster TPW speed. This trend would be caused by the elastic support of the upper high-viscosity part over the LVL. Indeed, if the LVL layer is regarded as liquid, its shape tends to follow the change of the centrifugal potential with no rigidity, and therefore deforms much more easily. At the same time, however, the upper part resists this liquid-like deformation. If the LVL depth is shallower, it means that the suppressing effect due to the upper part is weaker. Moreover, if its depth becomes sufficiently shallower, the elastic support becomes almost negligible. This is probably the main reason why the T_1 curves for the LVL models even with the different depths (i.e., between R1 and R2, and also R1′ and R2′) also approaches the same value for the variable upper mantle given here.

The above dependence on the LVL models is more clearly demonstrated in the time evolution of the viscoelastic tidal Love number in Fig. 2 (a1) and (b1). These results illustrate the viscoelastic deformation with respect to the shallowest and deepest LVL models (i.e., R1 and R5, respectively, chosen as typical examples), in response to constant external forcing defined as the Heaviside function. The deepest one is similar to Fig. 8 of Nakada and Okuno (2013). In both of the R1 and R5 models, a lower LVL viscosity results in a faster viscoelastic deformation. It is also obvious that the relaxation for the R1 model is much faster than that for the R5 model.

However, it should be noted that the dependence of T_1 on the LVL viscosity seen in Fig. 1 is not necessarily consistent with that of the Love number seen in Fig. 2 (a1) and (b1). For example, considering the R1 model, although T_1 of 10^{21} Pa·s is more than two factors of magnitude larger than that of 10^{19} Pa·s, such a strong dependence can not be found in the time evolution shown in Fig. 2 (a1). The reason is probably that the major relaxation modes are dominant in the time variation of the Love number (especially the M0 and C0 modes), whereas the minor relaxation modes with their extremely long timescale (especially the M1 and L0 modes) mainly governs T_1 as has been suggested by several previous parameter studies (e.g., Ricard et al., 1993; Vermeersen et al., 1997; Mitrovica and Milne, 1998; Nakada, 2000). Actually, as shown in Fig. 2 (a2), at the timespan after the major relaxation (approximately from 10^6 to 10^7 years), the subsequent time variation due to the minor relaxation becomes faster with the LVL viscosity reduction from 10^{21} Pa·s to 10^{19} Pa·s while it remains almost constant for LVL viscosity values lower than 10^{19} Pa·s. This tendency is consistent with the viscosity dependence of T_1 in Fig. 1 (a). On the other hand, considering the R5 model shown in Fig. 2 (b2), there is no clear difference among the results for the different viscosity values over the same timespan. Moreover, the lower viscosity provides the larger modal strength in this timespan. This trend means that, considering the weighting effect of the relaxation strengths, there is a positive effect on T_1 at a lower LVL viscosity. Nevertheless, the actual dependence of T_1 on the LVL viscosity is opposite as in Fig. 1 (b). Consequently, not only the slower relaxation mode but also the faster one should contribute to T_1.

The above-mentioned deference between the faster and slower modes regarding T_1 can be clearly seen also in dependence of each modes on the LVL viscosity (see $-1/s_i$, $-k_i/s_i$, and $k_i/k_f s_i^2$ for R1 and R5 in Fig. 3). Actually, variation of each relaxation strengths is not so simple because one mode sometimes tends to partly absorb another mode. This tendency is particularly remarkable when one relaxation timescale approaches another relaxation timescale depending on the parameter sweep. But still, the comparison between Fig. 3 (a1), (a2), and (a3) for R1, or (b1), (b2), and (b3) for R5, allow us to find that the two modes with the first and/or second longest relaxation timescales always have largest contribution to T_1 among all the modes. These two modes correspond to M1 and L0, related to the transition zone and the elastic lithosphere, respectively. Although both of the relaxation strengths of these two modes is not the largest, the weighted timescales in T_1 are still relatively long, reflecting the longest relaxation timescales. On the other hand, the modes with the larger relaxation strengths like M0 related to the whole mantle and C0 related to the liquid core do not make the largest contribution. However, for R5, the weighted timescale of C0 is longer than that of L0. This difference between R1 and R5 is probably because the shallower LVL interacts more with the lithosphere whereas the deeper LVL interacts more with the core.

4.2. Possible implication from the present results

The present parameter study tells us the non-negligible LVL effect on T_1 for the large-scale and long-term TPW of the Earth under the quasi-fluid approximation. In particular, if the LVL exists at about the top of the mantle, its effect largely reduces T_1 depending on the thickness, even less than about a half of that without any LVL. In general, not limited to the LVL, the low-viscosity part inside the mantle makes the TPW speed more or less faster. For example, most of the previous sensitivity analyses on the large-scale TPW (Spada et al., 1992a; Spada et al., 1993; Spada et al., 1996; Ricard et al., 1993; Richards et al., 1997; Richards et al., 1999; Greff-Lefftz, 2004; Greff-Lefftz, 2011; Nakada, 2007; Nakada, 2008; Creveling et al., 2012; Chan et al., 2014) have already investigated the dependence of the characteristic timescale and/or time evolution on the viscosity contrast between the upper and lower parts of the mantle. Still, considering the dependence on the LVL effect, the two-layered viscosity model might be too simplified to infer the

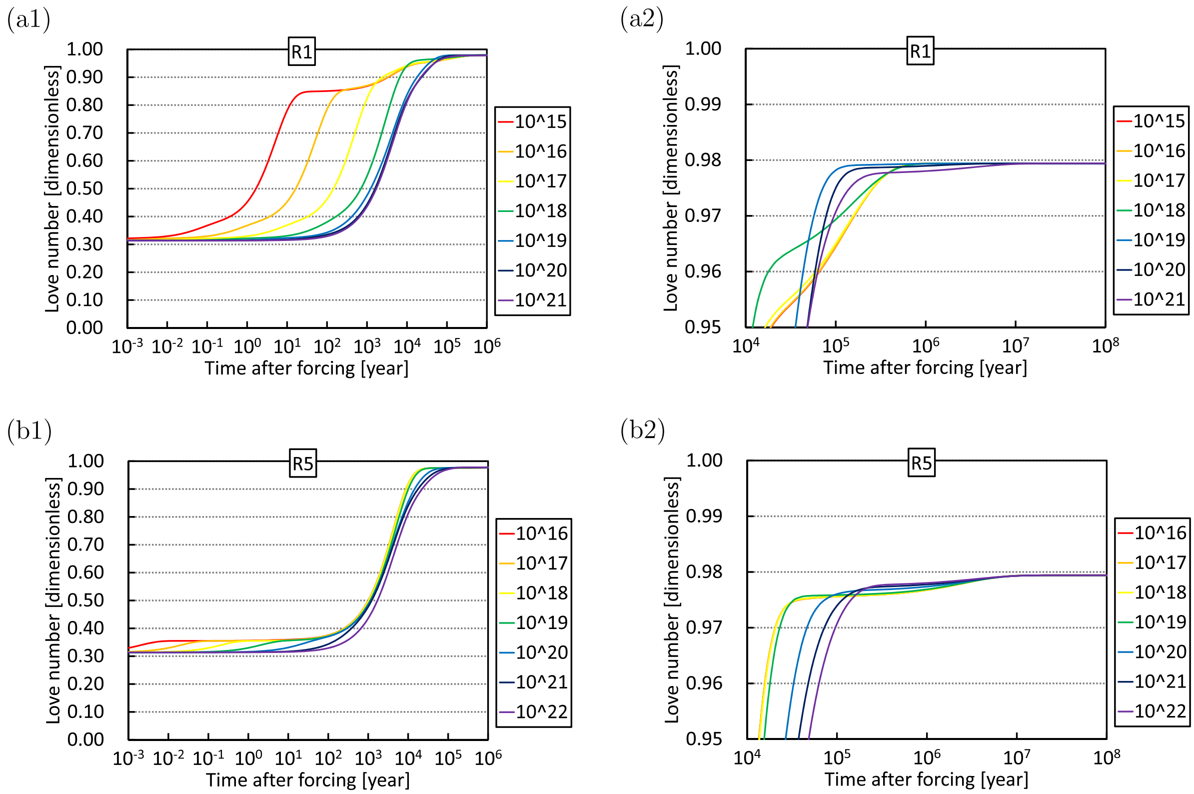

Fig. 2. (a1) Time evolution of the viscoelastic tidal Love number for the shallowest low-viscosity layer model R1 among Table 2 (a) in response to a constant external forcing expressed as the Heaviside function. (b1) Same as (a1) but for the deepest low-viscosity layer model R5. (a2) A close-up of (a1) at the end of its timespan. (b2) A close-up of (b1) at the end of its timespan.

viscosity structure by comparing the data-derived and model-derived TPW scenarios (cf., Creveling et al., 2012).

The reduction of the TPW timescale due to the LVL is almost proportional to the reduction of T_1 when the viscoelastic readjustment is dominant. In such a condition, the fact that the T_1 timescale becomes less than half means that the resultant TPW timescale also becomes less than half under the LVL effect. As explicitly derived in Harada (2012), particularly in the first and second terms of Eqs. (110) and (111), if the timescale of the load evolution is relatively shorter, the total TPW timescale mainly reflects the effect of the viscoelastic delay including consideration of the load amplitude. Otherwise, the TPW timescale just reflects that of the loading, that is, the rotational adjustment is almost always hydrostatic with no viscoelastic delay.

How about the large-scale TPW driven by temporary loading? As one example, apart from linear loading as derived in Spada et al. (1996) and Harada (2012), suppose that the quasi-fluid TPW due to oscillatory loading expressed as follows:

$$\beta(t) = \begin{cases} (\bar{\beta}/2)[1-\cos(2\pi t/\tau)] & \text{if} \quad 0 \leqslant t < \tau \\ 0 & \text{if} \quad t \geqslant \tau, \end{cases} \tag{1}$$

where t is time, β is normalized excitation, $\bar{\beta}$ is its maximum value, and τ is duration of excitation. These definitions are the same as those in Harada (2012) except for $\bar{\beta}$, which was defined as its final value in Harada (2012). The feature of this excitation is not exactly the same but somewhat similar to that discussed in Creveling et al. (2012). For the sake of simplification, the stabilizing effect of the fossil shape in the elastic lithosphere (e.g., Harada, 2012; Creveling et al., 2012; Chan et al., 2014) is ignored, for example, considering the case where the lithosphere has been completely broken and lost its remnant bulge. This assumption might let us underestimate the stabilization of the lithosphere (cf., Matsuyama et al., 2007). But still, it would enable us to understand the behavior of the solution more easily like that discussed in Harada (2012), by deriving the analytic solution:

$$\psi(t) = \bar{\alpha} - \begin{cases} \arctan\left\{\exp\left[\bar{\beta}\frac{t/\tau-(1/2\pi)\sin(2\pi t/\tau)}{T_1/\tau}\right]\tan\bar{\alpha}\right\} & \text{if} \quad 0 \leqslant t < \tau \\ \arctan\left\{\exp\left[\bar{\beta}\frac{1}{T_1/\tau}\right]\tan\bar{\alpha}\right\} & \text{if} \quad t \geqslant \tau, \end{cases} \tag{2}$$

where ψ is a resultant TPW angle and $\bar{\alpha}$ is an initial load location as an angular distance between the load and the original spin pole. These definitions are also the same as those in Harada (2012). It is obvious from the above solution that the TPW timescale is governed by the parameter $\bar{\beta}\tau/T_1$ although this parameter can be seen in the linear loading (e.g., Harada, 2012).

The dependence of the TPW angle on T_1 for oscillatory loading is basically similar to that for linear loading. As in Fig. 4 (a1) and (a2), if this parameter is large enough to make the rotation pole reach the equilibrium position:

$$\lim_{t\to\tau}\psi(t) = \bar{\alpha} - \frac{\pi}{2}, \tag{3}$$

the smaller this parameter is, the longer the timescale to reach the equilibrium position is. If not, however, it is possible that the spin pole will never reach the equilibrium state since the temporary loading finishes before the complete excursion of the pole. For such a case, as in Fig. 4 (b1) and (b2), the smaller this parameter is, the smaller the final TPW angle is. In either case, depending on how long T_1 within $\bar{\beta}\tau/T_1$ is, the time evolution of the TPW angle differs accordingly.

The TPW timescale does not show such simple dependence as interpreted above if the loading timescale is nearly comparable

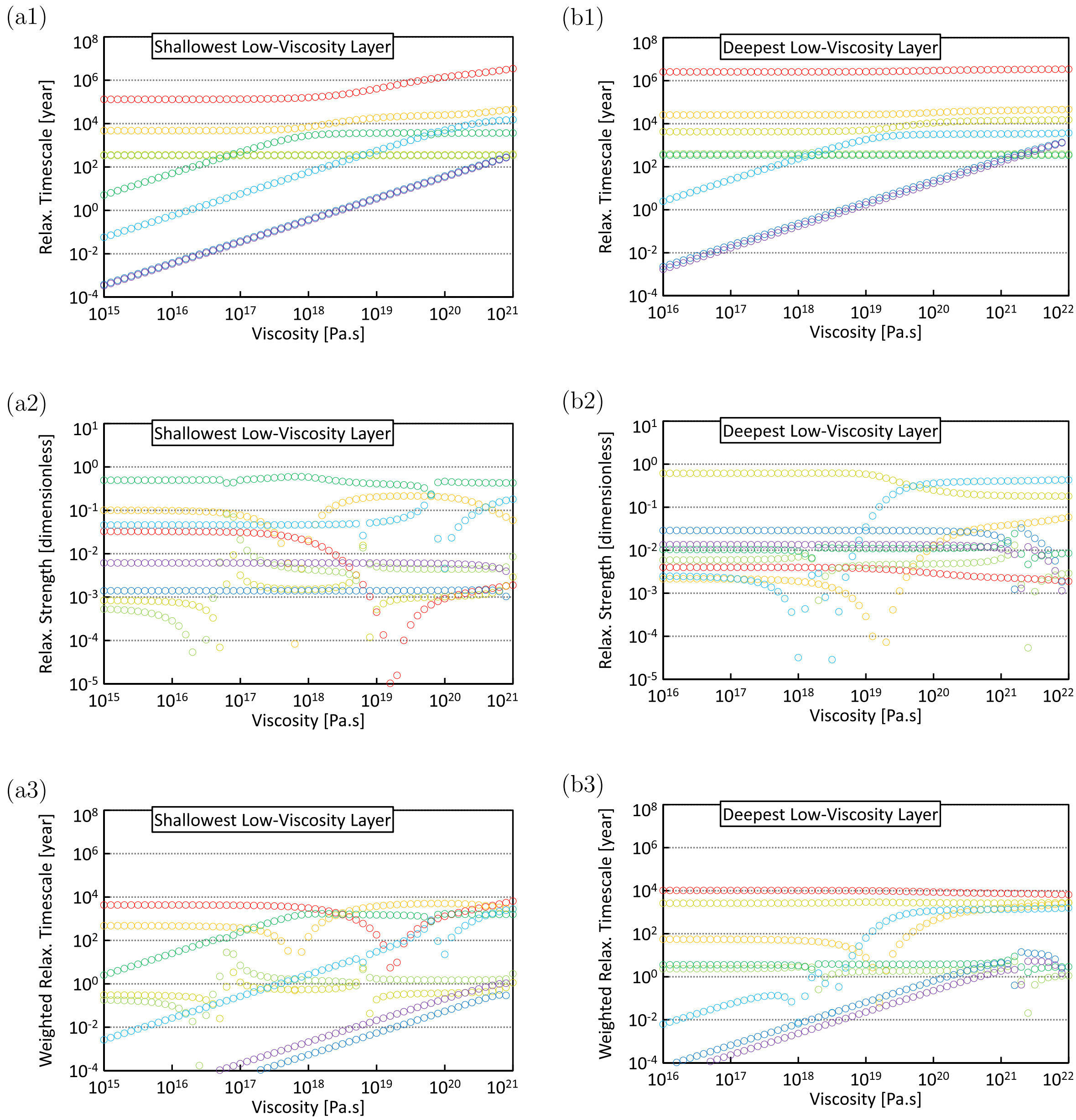

Fig. 3. (a1) Dependence of each relaxation timescales $-1/s_i$ on viscosity of a low-viscosity part for the shallowest low-viscosity layer model R1 among Table 2 (a). Each plots have different colors for the sake of comparison with the other two panels shown below. (a2) Same as (a1) but for the relaxation strengths $-k_i/s_i$. (a3) Same as (a1) but for the weighted relaxation timescales $k_i/k_f s_i^2$ which contribute to the characteristic timescale T_1 of true polar wander. (b1) Same as (a1) but for the deepest low-viscosity layer model R5. (b2) Same as (a2) but for the deepest low-viscosity layer model R5. (b3) Same as (a3) but for the deepest low-viscosity layer model R5.

to that of the viscous relaxation. This case also means that the validity of the quasi-fluid approximation is not always guaranteed, such as the secular polar motion driven by the GIA process. As introduced already, in the previous parameter studies on the small-scale and short-term TPW, Milne et al. (1998) found the effect of the shallow LVL on the TPW speed to be almost negligible (see their Fig. 4) while Nakada and Okuno (2013) found that of the deeper LVL to be non-negligible (see their Fig. 2). Although our results are inconsistent with both of their results, it is not so easy to compare ours with theirs since the TPW timescale dealt with in our analysis is much longer than that in their analyses. Probably, as Nakada and Okuno (2013) commented, the sensitivity of the GIA-induced TPW speed to the LVL viscosity might be quite different from that of the quasi-fluid TPW mostly explained by T_1, especially by the contribution of the slow M1 mode.

Perhaps the above difference between the short-term TPW in the previous analyses and the long-term TPW in this analysis is simply explainable by considering the relaxation modes demonstrated in Fig. 3. In the case of the short-term TPW, M1 is not effective because of its very small strength and also very long timescale. As a result, other than M0, L0 or C0 is expected to be effective for the shallower or deeper LVL (e.g., R1 or R5), respectively, in terms of both the relaxation timescales (i.e., smaller $-1/s_i$) and strengths (i.e., $-k_i/s_i$). For example, Milne et al. (1998) considered the shallower LVL in the viscosity range of about $10^{18.5}$ to $10^{20.5}$ Pa·s. This range does not show us any large variation in the relaxation timescale of L0. As shown in Fig. 3 (a1), the timescale is longer than 10^5 years, which is relatively long considering the typical GIA timescale. On the other hand, Nakada and Okuno (2013) considered the deeper LVL of 10^{18} to 10^{20} Pa·s. This range gives us some

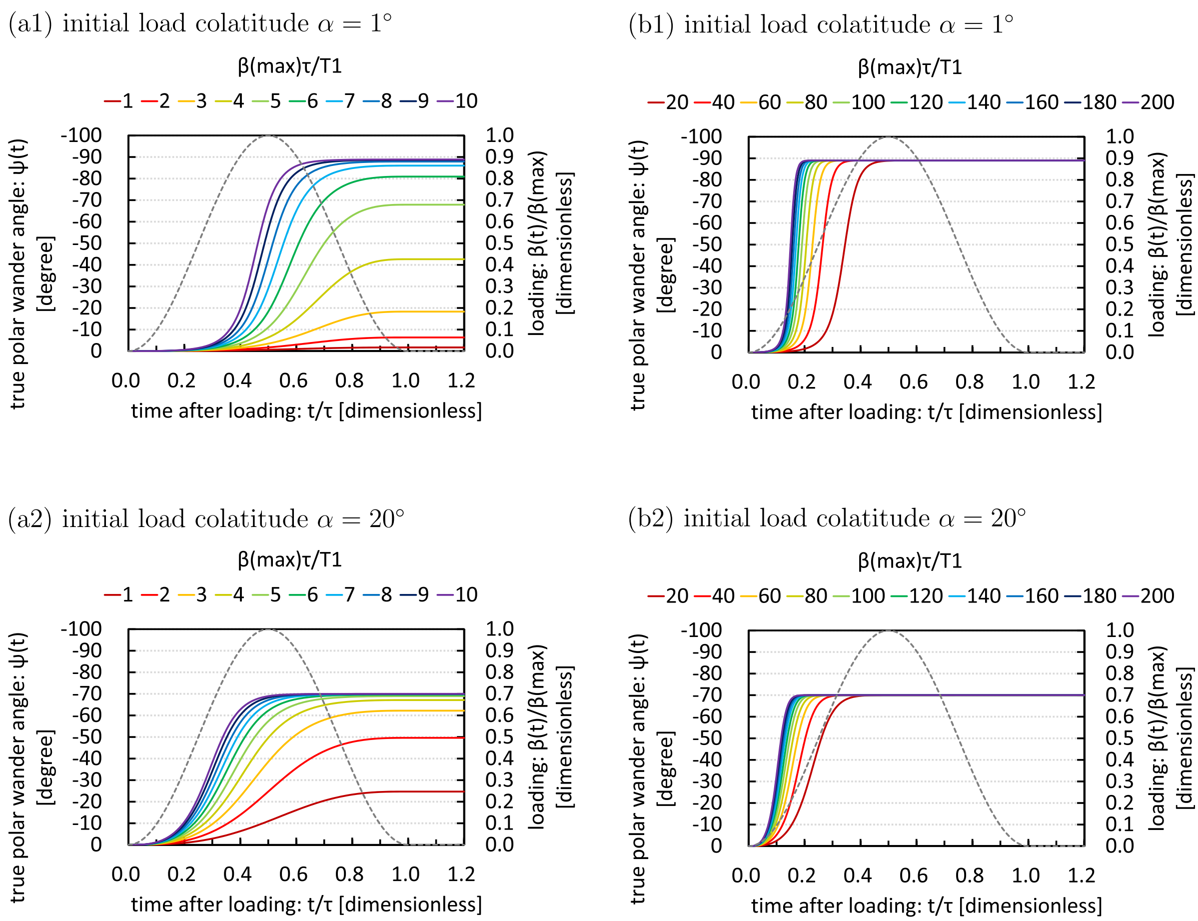

Fig. 4. Time variation of a hypothetical true polar wander angle (the left vertical axis with the solid curves) as a function of time (the horizontal axis) due to oscillatory loading (the right vertical axis with the dashed curve). For the sake of convenience, the sign of the vertical axis is replaced because the signs of the initial load colatitude and the load size are set only as positive for simplification. Also, the horizontal and right vertical axes are normalized by the timescale of load formation and the maximum of load evolution, respectively. The ten different colors of the curves represent a dimensionless quantity which controls how fast the viscoelastic readjustment of the rotational bulge is.

reduction in the relaxation timescale of C0 with the LVL viscosity. This timescale is mostly shorter than 10^5 years as shown in Fig. 3 (b1). At least qualitatively, these trends might explain that Milne et al. (1998) found almost no dependence on the shallower LVL and that Nakada and Okuno (2013) found the non-negligible dependence on the deeper LVL. In contrast to the short-term TPW, the contribution from M0 and C0 is no longer dominant for the long-term TPW discussed here since their relaxation timescales are too short to stabilize the rotation. In this case, M1 and L0 with longer timescales contribute to the stabilization dominantly. As a consequence, the dependence on the LVL depth for the long-term cases would be opposite to that for the short-term cases since the shallower or deeper LVL affects M1 and L0 more or less, respectively.

4.3. Open questions in the present study

For the sake of numerical convenience, the baseline structure in this study has two assumptions, that is, no viscoelastic lithosphere and no compressibility. These ideal cases should be reconsidered in addition to the LVL effect. Concerning the former assumption, Nakada (2000) previously examined the effect of the lithosphere which is not purely elastic. In such a case, there is the possibility of the interaction between the modes associated with density contrasts inside the mantle (e.g., M1) and those related to a viscoelastic lithosphere. On the latter assumption, it is difficult to solve the eigenvalue problem in the framework of the classical normal modes. There are some exceptional cases which escape this numerical difficulty through some specific treatments. For example, Nakada (2002), Nakada and Okuno (2003), and Nakada (2009) employed the iteration scheme to integrate the linear Liouville equation by using the time domain approach (Hanyk et al., 1995; Hanyk et al., 1996; Hanyk et al., 1999; Kamata et al., 2012; Kamata et al., 2013), which has been also applied to the non-linear Liouville equation (Nakada, 2007; Nakada, 2008). On the other hand, Cambiotti et al. (2010) handled the linear Liouville equation based on the continuous relaxation spectrum via the complex integral (Fang and Hager, 1994; Fang and Hager, 1995; Tanaka et al., 2006; Tanaka et al., 2007; Cambiotti and Sabadini, 2010). In order to investigate more realistic conditions, these treatments would be more robust than the classical normal mode method.

The main subject in this study was only the LVL effect on the Earth's TPW. However, a possible viscosity structure with an LVL-like heterogeneity might likewise affect Mars' TPW (cf., Spada et al., 1996; Rouby et al., 2008; Harada, 2012; Chan et al., 2014). Indeed, one of the above parameter studies (Chan et al., 2014, e.g., Fig. 10) demonstrated that the viscoelastic delay of the rotational response on Mars is unimportant for the loading timescale longer than about 10^6 years so that Martian rotation pole almost follows the load evolution. However, another one (Harada, 2012, e.g., Fig. 5) implied that the viscoelastic delay is effective if the load amplitude is almost canceled by the possible non-hydrostatic flattening stored in its elastic lithosphere. From this point of view, it might be still worth considering the possible LVL effect on Mars.

4.4. Final remarks

We conclude that the LVL inside the Earth's mantle potentially has a strong impact on T_1, especially if the LVL exists at the top of the mantle. In the previous modeling at least on the large-scale and long-term TPW, the viscosity structure of the Earth's mantle is largely simplified with no LVL effect. Here we calculated and discussed the LVL effect on the TPW timescale. Although the LVL effect has already been investigated from the viewpoint of the small-scale and short-term TPW, our result implies that, as formerly anticipated, the sensitivity to the LVL over the long timespan is not the same as that of the short timespan.

Acknowledgments

Two anonymous reviewers made many constructive comments on this manuscript. Thomas L. Wright helped us to improve this manuscript by correcting our English usage. This work was supported by China Postdoctoral Science Foundation (Grant No. 2013M542083) and the National Natural Science Foundation of China (Grant No. 41373066).

References

Bills, B.G., James, T.S., 1997. Polar motion of a viscoelastic Earth due to glacial cycle mass loading. J. Geophys. Res. Solid Earth 102 (B4), 7579–7602.
Bills, B.G., Neumann, G.A., Smith, D.E., Zuber, M.T., 2005. Improved estimate of tidal dissipation within Mars from MOLA observations of the shadow of Phobos. J. Geophys. Res. Planet. 110 (E7). http://dx.doi.org/10.1029/2004JE002376.
Boutin, D., Arkani-Hamed, J., 2006. Pole wandering of Mars: evidence from paleomagnetic poles. Icarus 181 (1), 13–25.
Cambiotti, G., Sabadini, R., 2010. The compressional and compositional stratifications in Maxwell earth models: the gravitational overturning and the long-period tangential flux. Geophys. J. Int. 180 (2), 475–500.
Cambiotti, G., Ricard, Y., Sabadini, R., 2010. Ice age true polar wander in a compressible and non-hydrostatic. Earth Geophys. J. Int. 183 (3), 1248–1264.
Chan, N.-H., Mitrovica, J.X., Daradich, A., Creveling, J.R., Matsuyama, I., Stanley, S., 2014. Time-dependent rotational stability of dynamic planets with elastic lithospheres. J. Geophys. Res. Planet. 119 (1), 169–188.
Creveling, J.R., Mitrovica, J.X., Chan, N.H., Latychev, K., Matsuyama, I., 2012. Mechanisms for oscillatory true polar wander. Nature 491 (7423), 244–248.
Dixon, J.E., Dixon, T.H., Bell, D.R., Malservisi, R., 2004. Lateral variation in upper mantle viscosity: role of water. Earth Planet. Sci. Lett. 222 (2), 451–467.
Dziewonski, A.M., Anderson, D.L., 1981. Preliminary reference Earth model. Phys. Earth Planet. In. 25 (4), 297–356.
Fang, M., Hager, B.H., 1994. A singularity-free approach to post glacial rebound calculations. Geophys. Res. Lett. 21 (19), 2131–2134.
Fang, M., Hager, B.H., 1995. The singularity mystery associated with a radially continuous Maxwell viscoelastic structure. Geophys. J. Int. 123 (3), 849–865.
Forte, A.M., Mitrovica, J.X., 2001. Deep-mantle high-viscosity flow and thermochemical structure inferred from seismic and geodynamic data. Nature 410 (6832), 1049–1056.
Gilbert, F., Dziewonski, A.M., 1975. Application of normal mode theory to retrieval of structural parameters and source mechanisms from seismic spectra. Philos. Transact. Roy. Soc. A 278 (1280), 187–269.
Greff-Lefftz, M., 2004. Upwelling plumes, superswells and true polar wander. Geophys. J. Int. 159 (3), 1125–1137.
Greff-Lefftz, M., 2011. Length of day variations due to mantle dynamics at geological timescale. Geophys. J. Int. 187 (2), 595–612.
Hanyk, L., Moser, J., Yuen, D.A., Matyska, C., 1995. Time-domain approach for the transient responses in stratified viscoelastic Earth models. Geophys. Res. Lett. 22 (10), 1285–1288.
Hanyk, L., Yuen, D.A., Matyska, C., 1996. Initial-value and modal approaches for transient viscoelastic responses with complex viscosity profiles. Geophys. J. Int. 127 (2), 348–362.
Hanyk, L., Matyska, C., Yuen, D.A., 1999. Secular gravitational instability of a compressible viscoelastic sphere. Geophys. Res. Lett. 26 (5), 557–560.
Harada, Y., 2012. Long-term polar motion on a quasi-fluid planetary body with an elastic lithosphere: semi-analytic solutions of the time-dependent equation. Icarus 220 (2), 449–465.
Hearn, E.H., 2003. What can gps data tell us about the dynamics of post-seismic deformation? Geophys. J. Int. 155 (3), 753–777.
Hood, L.L., Young, C.N., Richmond, N.C., Harrison, K.P., 2005. Modeling of major martian magnetic anomalies: further evidence for polar reorientations during the noachian. Icarus 177 (1), 144–173.
Kamata, S., Sugita, S., Abe, Y., 2012. A new spectral calculation scheme for long-term deformation of Maxwellian planetary bodies. J. Geophys. Res. Planet. 117. http://dx.doi.org/10.1029/2011JE003945.
Kamata, S., Sugita, S., Abe, Y., Ishihara, Y., Harada, Y., Morota, T., Namiki, N., Iwata, T., Hanada, H., Araki, H., Matsumoto, K., Tajika, E., 2013. Viscoelastic deformation of lunar impact basins: implications for heterogeneity in the deep crustal paleo-thermal state and radioactive element concentration. J. Geophys. Res. Planet. 118 (3), 398–415.
Kawakatsu, H., Kumar, P., Takei, Y., Shinohara, M., Kanazawa, T., Araki, E., Suyehiro, K., 2009. Seismic evidence for sharp lithosphere-asthenosphere boundaries of oceanic plates. Science 324 (5926), 499–502.
Klein, A., Jacoby, W., Smilde, P., 1997. Mining-induced crustal deformation in northwest Germany: modelling the rheological structure of the lithosphere. Earth Planet. Sc. Lett. 147 (1-4), 107–123.
Lambeck, K., 1980. The Earth's Variable Rotation: Geophysical Causes and Consequences. Cambridge Univ. Press, London.
Langlais, B., Quesnel, Y., 2008. New perspectives on Mars' crustal magnetic field. C.R. Geosci. 340 (12), 791–800.
Maloof, A.C., Halverson, G.P., Kirschvink, J.L., Schrag, D.P., Weiss, B.P., Hoffman, P.F., 2006. Combined paleomagnetic, isotopic, and stratigraphic evidence for true polar wander from the Neoproterozoic Akademikerbreen Group, Svalbard, Norway. Geol. Soc. Am. Bull. 118 (9-10), 1099–1124.
Matsuyama, I., Mitrovica, J.X., Manga, M., Perron, J.T., Richards, M.A., 2006. Rotational stability of dynamic planets with elastic lithospheres. J. Geophys. Res. Planet. 111 (E2). http://dx.doi.org/10.1029/2005JE002447.
Matsuyama, I., Nimmo, F., Mitrovica, J.X., 2007. Reorientation of planets with lithospheres: the effect of elastic energy. Icarus 191 (2), 401–412.
Milne, G.A., Mitrovica, J.X., Forte, A.M., 1998. The sensitivity of glacial isostatic adjustment predictions to a low-viscosity layer at the base of the upper mantle. Earth Planet. Sci. Lett. 154 (1-4), 265–278.
Mitchell, R.N., Evans, D.A.D., Kilian, T.M., 2010a. Rapid early Cambrian rotation of Gondwana. Geology 38 (8), 755–758.
Mitchell, R.N., Hoffman, P.F., Evans, D.A.D., 2010b. Coronation loop resurrected: oscillatory apparent polar wander of Orosirian (2.05–1.8 Ga) paleomagnetic poles from Slave craton. Precambrian Res. 179 (1-4), 121–134.
Mitrovica, J.X., Forte, A.M., 2004. A new inference of mantle viscosity based upon joint inversion of convection and glacial isostatic adjustment data. Earth Planet. Sci. Lett. 225 (1-2), 177–189.
Mitrovica, J.X., Milne, G.A., 1998. Glaciation-induced perturbations in the Earth's rotation: a new appraisal. J. Geophys. Res. Solid Earth 103 (B1), 985–1005.
Munk, W.H., MacDonald, G.J.F., 1960. The Rotation of the Earth. Cambridge Univ. Press, New York.
Nakada, M., 2000. Effect of the viscoelastic lithosphere on polar wander speed caused by the late Pleistocene glacial cycles. Geophys. J. Int. 143 (1), 230–238.
Nakada, M., 2002. Polar wander caused by the Quaternary glacial cycles and fluid Love number. Earth Planet. Sci. Lett. 200 (1-2), 159–166.
Nakada, M., 2007. True polar wander associated with continental drift on a hypothetical Earth. Earth Planets Space 59 (6), 513–522.
Nakada, M., 2008. Long-term true polar wander of the Earth including the effects of convective processes in the mantle and continental drift. Geophys. J. Int. 175 (3), 1235–1244.
Nakada, M., 2009. Polar wander of the Earth associated with the Quaternary glacial cycle on a convecting mantle. Geophys. J. Int. 179 (1), 569–578.
Nakada, M., Karato, S., 2012. Low viscosity of the bottom of the Earth's mantle inferred from the analysis of Chandler wobble and tidal deformation. Phys. Earth Planet. In. 192, 68–80.
Nakada, M., Okuno, J., 2003. Perturbations of the Earth's rotation and their implications for the present-day mass balance of both polar ice caps. Geophys. J. Int. 152 (1), 124–138.
Nakada, M., Okuno, J., 2013. GIA-related rotational variations for the Earth with low-viscosity D″ layer. Geophys. J. Int. 195 (2), 725–739.
Nakada, M., Iriguchi, C., Karato, S., 2012. The viscosity structure of the D″ layer of the Earth's mantle inferred from the analysis of Chandler wobble and tidal deformation. Phys. Earth Planet. In. 208, 11–24.
Ogawa, M., Yanagisawa, T., 2012. Two-dimensional numerical studies on the effects of water on Martian mantle evolution induced by magmatism and solid-state mantle convection. J. Geophys. Res. Planet., 117.
Peltier, W.R., 1974. Impulse response of a Maxwell Earth. Rev. Geophys. 12 (4), 649–669.
Pollitz, F.F., 2003. Transient rheology of the uppermost mantle beneath the Mojave Desert, California. Earth Planet. Sc. Lett. 215 (1-2), 89–104.
Ricard, Y., Spada, G., Sabadini, R., 1993. Polar wandering of a dynamic Earth. Geophys. J. Int. 113 (2), 284–298.
Richards, M.A., Ricard, Y., Lithgow-Bertelloni, C., Spada, G., Sabadini, R., 1997. An explanation for Earth's long-term rotational stability. Science 275 (5298), 372–375.
Richards, M.A., Bunge, H.P., Ricard, Y., Baumgardner, J.R., 1999. Polar wandering in mantle convection models. Geophys. Res. Lett. 26 (12), 1777–1780.
Rouby, H., Greff-Lefftz, M., Besse, J., 2008. Rotational bulge and one plume convection pattern: Influence on Martian true polar wander. Earth Planet. Sci. Lett. 272 (1-2), 212–220.
Sabadini, R., Yuen, D.A., Boschi, E., 1984. A comparison of the complete and truncated versions of the polar wander equations. J. Geophys. Res. 89 (B9), 7609–7620.
Spada, G., Ricard, Y., Sabadini, R., 1992a. Excitation of true polar wander by subduction. Nature 360 (6403), 452–454.
Spada, G., Sabadini, R., Yuen, D.A., Ricard, Y., 1992b. Effects on postglacial rebound from the hard rheology in the transition zone. Geophys. J. Int. 109 (3), 683–700.

Spada, G., Sabadini, R., Ricard, Y., 1993. On a particular solution of the nonlinear Liouville equations. Geophys. J. Int. 114 (2), 399–404.
Spada, G., Sabadini, R., Boschi, E., 1996. Long-term rotation and mantle dynamics of the Earth, Mars, and Venus. J. Geophys. Res. Planet. 101 (E1), 2253–2266.
Sprenke, K.F., Baker, L.L., 2000. Magnetization, paleomagnetic poles, and polar wander on Mars. Icarus 147 (1), 26–34.
Steffen, H., Kaufmann, G., 2005. Glacial isostatic adjustment of Scandinavia and northwestern Europe and the radial viscosity structure of the Earth's mantle. Geophys. J. Int. 163 (2), 801–812.
Steinberger, B., Torsvik, T.H., 2008. Absolute plate motions and true polar wander in the absence of hotspot tracks. Nature 452 (7187), 620–623.
Tanaka, Y., Okuno, J., Okubo, S., 2006. A new method for the computation of global viscoelastic post-seismic deformation in a realistic earth model (i) – vertical displacement and gravity variation. Geophys. J. Int. 164 (2), 273–289.
Tanaka, Y., Okuno, J., Okubo, S., 2007. A new method for the computation of global viscoelastic post-seismic deformation in a realistic earth model (ii) – horizontal displacement. Geophys. J. Int. 170 (3), 1031–1052.
Torsvik, T.H., Van der Voo, R., Preeden, U., Mac Niocaill, C., Steinberger, B., Doubrovine, P.V., van Hinsbergen, D.J.J., Domeier, M., Gaina, C., Tohver, E., Meert, McCausland, P.J.A., Cocks, L.R.M., 2012. Phanerozoic polar wander, palaeogeography and dynamics. Earth Sci. Rev. 114 (3-4), 325–368.
Tsai, V.C., Stevenson, D.J., 2007. Theoretical constraints on true polar wander. J. Geophys. Res. Solid Earth 112 (B5). http://dx.doi.org/10.1029/2005JB003923.
Van der Voo, R., 1994. True polar wander during the middle Paleozoic? Earth Planet. Sci. Lett. 122 (1-2), 239–243.
Vermeersen, L.L.A., Sabadini, R., Spada, G., 1996. Analytical visco-elastic relaxation models. Geophys. Res. Lett. 23 (7), 697–700.
Vermeersen, L.L.A., Fournier, A., Sabadini, R., 1997. Changes in rotation induced by Pleistocene ice masses with stratified analytical Earth models. J. Geophys. Res. Solid Earth 102 (B12), 27689–27702.
Willemann, R.J., 1984. Reorientation of planets with elastic lithospheres. Icarus 60 (3), 701–709.
Wu, P., Peltier, W.R., 1982. Viscous gravitational relaxation. Geophys. J. Roy. Astron. Soc. 70 (2), 435–485.
Yuen, D.A., Sabadini, R., Boschi, E., 1983. The dynamical equations of polar wander and the global characteristics of the lithosphere as extracted from rotational data. Phys. Earth Planet. In. 33 (3), 226–242.